Effect of Short Chain Branching on the Coil Dimensions of Polyolefins in Dilute Solution

Thomas Sun* and Patrick Brant

Baytown Polymers Center, ExxonMobil Chemical Company, 5200 Bayway Dr., Baytown, Texas 77520-2101

Ronald R. Chance and William W. Graessley†

Corporate Stragetic Research, ExxonMobil Research and Engineering, Annandale, New Jersey 08801

Received April 26, 2001; Revised Manuscript Received June 26, 2001

ABSTRACT: This paper deals with the short branch effect in α-olefin copolymers on radius of gyration R_g and intrinsic viscosity $[\eta]$ in trichlorobenzene at 135 °C. A wide range of structurally uniform copolymers of ethylene with propylene, 1-butene, 1-hexene, and 1-octene were analyzed by size exclusion chromatography with on-line refractive index, low-angle and multiangle light-scattering and viscometry detectors. Variation of refractive index increment with composition was determined, and corrections for finite concentration were applied. Both R_g and $[\eta]$ are accurately described by power laws $R_g = K_s M^{\alpha_s}$ and $[\eta] = K_v M^{\alpha_v}$. The coefficients K_s and K_v vary with comonomer type and amount, but the same exponents, $\alpha_s = 0.58$ and $\alpha_v = 0.695$, apply within the measurement uncertainty to all polymers studied. The ratios $g_{SCB} = R_g^2/(R_g^2)_{PE}$ and $g'_{SCB} = [\eta]/([\eta])_{PE}$ vary linearly with comonomer weight fraction, with slopes that depend on the comonomer type. Various explanations for the observations are considered.

Introduction

The importance of short chain branching (SCB) in the solid-state properties of ethylene homopolymers and α-olefin copolymers is well-known.[1,2] Stiffness, ductility, tear strength, clarity, and softening temperature are among the many performance characteristics affected profoundly by SCB structure, frequency and distribution. Among the analytical techniques used to characterize SCB are nuclear magnetic resonance (NMR) and Fourier transform infrared spectroscopy (FTIR) for comonomer content and sequencing[3,4] and temperature rising elution fractionation (TREF) for compositional uniformity.[5]

Large scale molecular architecture such as molecular weight distribution (MWD) and long chain branching (LCB) strongly influence the melt rheology and hence the processing behavior of polymers. Size exclusion chromatography (SEC),[6,7] which sorts polymer molecules according to size in dilute solution, is the method of choice for characterizing the large-scale architecture. Supported by various on-line detectors,[8] SEC provides the size-mass relationship needed to deduce information about MWD and LCB. Although SCB itself has little direct bearing on melt rheology, it does influence the size-mass relationship, and its contribution must be known in order to obtain a correct characterization of MWD and LCB. The aim of the work described here is to establish the size-mass contribution of SCB for copolymers of ethylene with propylene (EP), 1-butene (EB), 1-hexene (EH), and 1-octene (EO).

Of the 33 polyolefins in this study, 28 are copolymers, typically with molecular weight $M_w \sim 10^5$ and typically synthesized under conditions that favor both intramolecular and intermolecular uniformity in the comonomer incorporation statistics (e.g., metallocene-based catalysis[9]). The other five samples are homopolymers with molecular weights in the same range—high-density polyethylene and isotactic samples of polypropylene, poly(1-butene), poly(1-hexene), and poly(1-octene). Most samples have relatively narrow molecular weight distributions, $M_w/M_n \sim 2$, although a few are somewhat broader.

Two SEC configurations were used in the work, one with on-line refractive index and multiangle light-scattering detection (SEC−MALLS) and the other with refractive index, low-angle light-scattering, and viscometric detection (SEC−LALLS−VIS). The narrow distribution fractions emerging from the SEC columns were directed through detectors whose outputs were used to determine concentration c, molecular weight M, radius of gyration R_g, and intrinsic viscosity $[\eta]$ on a continuous basis. The solvent used in all cases was 1,2,4 trichlorobenzene (TCB) at 135 °C.

Experimental Section

Instrumentation. A Waters 150C high temperature SEC with three Polymer Laboratories PLgel 10 mm Mixed-B columns, a nominal flow rate of 0.5 cm^3/min, and a nominal injection volume of 300 μL is common to both detector configurations. The various transfer lines, columns, and differential refractometer (the DRI detector, used mainly to determine eluting solution concentrations) are contained in an oven maintained at 135 °C.

The MALLS detector is model DAWN DSP (Wyatt Technology, Inc.). The primary components are an optical flow cell, a 30 mW, 488 nm argon ion laser light source, and an array of 17 photodiodes placed at collection angles from 17.7 to 154.8°. A heated transfer line, maintained at 135 °C, conducts the stream emerging from the SEC columns out of the oven and into the optical flow cell (also maintained at 135 °C) and then back into the oven to the DRI detector.

The LALLS detector is the model 2040 dual-angle light-scattering photometer (Precision Detector Inc.). Its flow cell, located in the SEC oven, uses a 690 nm diode laser light source and collects scattered light at two angles, 15 and 90°. Only the 15° output was used in these experiments. Its signal is

† Present address: 7496 Old Channel Trail, Montague, MI 49437.

10.1021/ma010718e CCC: $20.00 © 2001 American Chemical Society
Published on Web 08/17/2001

Table 1. Molecular Structure of Polyolefin Samples

polymer	wt. % comonomer	$M_w \times 10^{-5}$ (SEC−MALLS)	M_w/M_n (DRI analysis)
HDPE	0	1.82	3.90
EP22	21.9	1.69	3.19
EP27	27.3	1.29	2.59
EP52	51.8	1.71	2.23
EP81	80.7	1.59	2.12
EP100	100	1.77	3.1
EB8	7.6	1.13	2.15
EB9	8.8	0.76	2.12
EB10	9.9	0.95	2.10
EB11	10.3	0.80	2.21
EB12	11.7	1.15	2.03
EB13	12.6	0.86	2.06
EB18	18.1	0.99	2.03
EB19	18.2	1.02	2.26
EB22	22.0	1.38	2.02
EB25	25.1	0.90	2.20
EB100	100	1.69	1.89
EH5	4.5	1.04	2.16
EH6	6.0	0.89	2.51
EH9	9.0	1.19	2.03
EH11	10.8	0.78	2.40
EH12	12.2	0.94	2.08
EH14	14.2	1.15	2.04
EH18	18.4	0.83	1.96
EH70	70.2	2.69	2.76
EH100	100	0.77	1.92
EO10	9.5	1.26	3.85
EO13	13.2	1.27	4.26
EO18	17.8	0.88	3.85
EO34	34.4	2.14	2.53
EO42	41.9	2.04	2.05
EO50	49.9	0.79	2.32
EO100	100	1.54	3.06

sent to a data acquisition board (National Instruments) that accumulates readings at a rate of 16 per second. The lowest four readings are averaged, and then a proportional signal is sent to the SEC−LALLS−VIS computer. The LALLS detector is positioned after the SEC columns, but before the viscometer.

The viscometer is a high-temperature Model 150R (Viscotek Corp.). It consists of four capillaries arranged in a Wheatstone bridge configuration with two pressure transducers. One transducer measures the total pressure drop across the detector, and the other, positioned between the two sides of the bridge, measures a differential pressure. The specific viscosity $\eta_{sp}(c) = (\eta(c) - \eta_s)/\eta_s$ for the solution then flowing through the viscometer is calculated from their outputs. The viscometer is inside the SEC oven, positioned after the LALLS detector but before the DRI detector.

Calibration. The DRI detector was calibrated by integrating the signal obtained by injecting a known quantity of NBS1475, a polyethylene standard.[10] The DRI response, directly proportional to the product of polymer concentration and refractive index increment $c(dn/dc)$, is discussed in some detail in the data analysis section.

The MALLS detector was calibrated by measuring the 90° scattering intensity of the elution solvent TCB at 135 °C. For these conditions, the Rayleigh ratio of TCB at 488 nm is 1.065×10^{-4} cm^{-1}. We normalized the photodetectors by injecting a low molecular weight polymer which scatters light nearly isotropically. The polymer used for this purpose was NBS1482, a polyethylene standard fraction with certificate $M_w = 13\,600$.[11] On the basis of extrapolations of our own and literature data for polyethylenes of higher molecular weight,[10,11] we estimate $R_g = 5$ nm for NBS1482. That size corresponds to an expected 1% asymmetry in scattering intensity between the lowest and highest scattering angles. The values of M_w for the polymers in this study, obtained by the SEC−MALLS method, are listed in Table 1. Also listed there are values of M_w/M_n, determined with the correlation of elution volume and molecular weight as furnished by the MALLS data.

The manufacturer suggests calibrating the LALLS detector by injecting a polymer sample of known molecular weight and adjusting the LS calibration constant accordingly. Using this method, we calibrated the LALLS detector such that the M_w value it measures matches the value obtained by the MALLS detector (on average) for the same sample. For the 33 samples studied we find an average discrepancy between the measured MALLS and LALLS values of 0.5% with a standard deviation of 1.5%. For comparison, the standard deviation over 12 measurements for M_w of the homopolyethylene control is 1.4% for the MALLS measurement and 2.1% for the LALLS measurement.

The viscometer was calibrated by injecting three standard polyethylenes (NBS1482, NBS1483, and NBS1484), for which $[\eta]$ in TCB at 130 °C is supplied with an expected limit of systematic error[11] of 1%. The viscometer calibration constant was then adjusted to match, on average, the stated intrinsic viscosity values. The results of those adjustments are shown in Table 2.

Interdetector volumes for the SEC−MALLS and SEC−LALLS−VIS configurations were determined by overlapping the refractive index, light-scattering, and viscometer chromatograms obtained for a narrow distribution polystyrene standard. The manufacturer-stated upper limit polydispersity for this sample is $M_w/M_n = 1.02$; with our column set we obtain a polydispersity of 1.05.

Operating Procedures. The elution solvent was prepared by adding approximate 1.5 g of the antioxidant BHT/L of reagent grade TCB (Aldrich), then filtering through a 0.7 μm glass prefilter followed by a 0.1 μm Teflon filter. Most of this solvent was used as the SEC mobile phase, with a small aliquot retained for polymer solution preparation. The solvent was passed through an on-line degasser (Phenomenex Model DG4000) before entering the SEC.

Polymer solutions were prepared by placing dry polymer in a glass container, adding the desired amount of TCB, then heating the mixture at 160 °C with continuous agitation for about 2 h. All quantities were measured gravimetrically. The TCB densities used to express the polymer concentration in mass/volume units are 1.463 g/cm^3 at room temperature and 1.324 g/cm^3 at 135 °C. The injection concentration c_o ranged from 1.0 to 2.0 mg/cm^3, with lower concentrations being used for higher molecular weight samples.

Sample Characterization. The determination of comonomer content for EB, EH, and EO samples relied primarily on proton NMR. The determination of comonomer content for EP samples primarily relied on an FTIR method calibrated by ^{13}C NMR. Comonomer contents are given in Table 1. Measurements of TREF demonstrated acceptable compositional uniformity in the EB and EH samples, as expected for metallocene-derived polymers. The EP samples could not be analyzed by TREF. Three of the EO samples, EO10, EO13, and EO18, are Ziegler−Natta products and somewhat nonuniform in composition distribution. However, this degree of nonuniformity did not significantly manifest itself in this SEC study.

Data Analysis

Basic Formalisms. The SEC−MALLS data were analyzed with the standard formulas for static light scattering,[12] treating the narrow distribution SEC fractions as monodisperse:

$$\frac{K_o c}{\Delta R(\theta,c)} = \frac{1}{MP(\theta)} + 2A_2 c \qquad (1)$$

Here, $\Delta R(\theta,c)$ is the excess Rayleigh scattering intensity at scattering angle θ, c is the polymer concentration, M is the polymer molecular weight, A_2 is the second virial coefficient of the solution, and $P(\theta)$ is the form factor for monodisperse, random coils

$$P(u) = \frac{2[\exp(-u) - 1 + u]}{u^2} \qquad (2)$$

Table 2. Comparison of Certificate Values of M_w and [η] for Polyethylene Standards with Averaged Measurements in This Study

standard	M_w (certificate)	M_w (SEC−MALLS)	[η], dL/g (certificate)	[η], dL/g (SEC−LALLS−VIS)
NBS 1482	13 600	12 600	0.402	0.395
NBS 1483	32 100	31 900	0.794	0.795
NBS 1484	119 600	122 100	1.979	2.010

in which

$$u = \frac{16\pi^2 n^2 R_g{}^2 \sin^2\theta/2}{\lambda^2} \tag{3}$$

The refractive index of solvent is n, λ is the in vacuo wavelength of incident light, and R_g is the polymer radius of gyration. In eq 1, K_o is the optical constant for the system

$$K_o = \frac{4\pi^2 n^2 (dn/dc)^2}{\lambda^4 N_A} \tag{4}$$

in which N_A is Avogadro's number, and dn/dc is the refractive index increment for the system. The concentrations used in the analyses are the values obtained from the DRI output. The values of dn/dc and A_2 for the various copolymers are discussed below. The MALLS data were analyzed with both the commercial Astra software (Wyatt Technologies) and in-house written software to extract M from the scattering intensity in the low angle scattering limit and R_g from the angular dependence of scattering intensity. The two analyses gave identical answers.

The LALLS data obtained from the SEC−LALLS−VIS configuration were analyzed according to eq 1 with the form factor set to unity. The error in M caused by this approximation would be ~2% for a molecule with $R_g = 70$ nm ($\theta = 15°$, $\lambda = 690$ nm), corresponding to a polyethylene molecule with $M \sim 10^6$. Errors for the polymers in this work, having molecular weights that range from about 70 000 to 300 000, would of course be smaller.

The viscometry data were analyzed with the Huggins equation[13]

$$\eta_{sp} = c[\eta] + k_H[\eta]^2 c^2 \tag{5}$$

where [η] is the intrinsic viscosity of the polymer, and k_H is the Huggins coefficient. The SEC−LALLS−VIS data were analyzed with in-house written software.

The above three equations describe how M, R_g and [η] are extracted from the experimental data. However, the data analysis requires knowledge of certain parameters, dn/dc and A_2 for light scattering and k_H for viscometry. The following three subsections discuss how we have determined the values used in the analyses and their effect on the results obtained.

Refractive Index Increment. Pope and Chu[14] report $dn/dc = -0.109$ cm^3/g ($\lambda = 488$ nm) for polyethylene in TCB at 135 °C. We have used this value to evaluate M_w for the polyethylene standards with the SEC−MALLS configuration. Table 2 compares the M_w values obtained (average over several runs) with the reported values.[11] An 11% limit of systematic error is claimed for the three polymers, and our values are well inside that range. The MALLS result is dependent on dn/dc but otherwise is an absolute determination of M_w, with no freely adjustable parameters. If the Pope−Chu dn/dc were significantly in error we would expect a larger discrepancy, particularly since the M_w value obtained is proportional to $(dn/dc)^2$. We thus accept and use $dn/dc = -0.109$ cm^3/g for linear polyethylene.

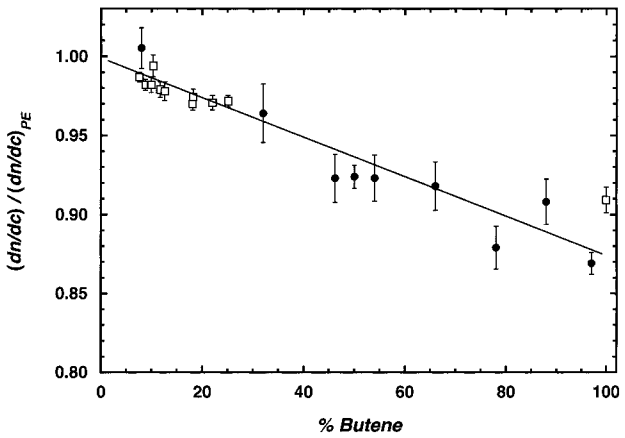

Figure 1. Composition dependence of the refractive index increment relative to polyethylene for ethylene-butene copolymers in TCB at 135 °C. The symbols indicate EB copolymers (□) and model EB's (●).

Having established a value of dn/dc for polyethylene, we now consider its dependence on copolymer content and type. Changes in dn/dc can be evaluated from the DRI response since the integrated area of the DRI signal for fixed injection volume is proportional to the product of stock solution concentration and refractive index increment:

$$A_{DRI} = \Lambda c_o \, dn/dc \tag{6}$$

in which Λ is an instrumental constant and thus independent of polymer species. If dn/dc changes with comonomer content or type, we would expect to find a corresponding change in the ratio A_{DRI}/c_o.

An extensive investigation of copolymer effects on dn/dc by this method revealed them to be small for the EP, EH and EO copolymers and of no consequence in the analysis to follow. For the EB copolymers, however, dn/dc does vary systematically with comonomer content and to a much greater extent than in the other copolymer series. Fortunately, a supply of model EB copolymers was available to examine the validity of this apparent difference from the other copolymer behavior. The model EB's were made by hydrogenating the double bonds of polybutadienes of various 1,2 (vinyl) contents. They are nearly monodisperse and from ^{13}C NMR have statistically uniform ethyl group sequencing.[15] Owing to the near-monodispersity of these polymers, slightly different methods of analysis are employed to determine their dilute solution properties and will be described separately.[16] As can be seen in Figure 1, the dn/dc results for the model materials and the EB copolymers of this work agree very well. The composition dependence is well described by a straight line

$$(dn/dc)_{EB} = (dn/dc)_{PE}\,(1-0.126w) \tag{7}$$

where w is the weight fraction of 1-butene. The slope −0.126 has a standard error estimate of about 5% in the linear fit. Similar plots of data for the EP, EH, and EO copolymers have much smaller slopes, arguably zero within the uncertainty of the measurements. In the analyses to follow, appropriate corrections for the variation of dn/dc with comonomer content are applied for EB copolymers and ignored as insignificant for the other systems. As explained elsewhere,[16] the anomalous behavior of dn/dc for the EB system appears understandable from the unusual variation in melt density with composition[17] and the Lorentz−Lorentz formulation of refractive index.[12]

Second Virial Coefficient. In dilute solution light scattering, A_2 contributes a second-order term whose relative importance is determined by the quantity $2A_2Mc$. The polymer concentrations eluting from SEC columns are typically low enough that this term may be neglected. However, polyolefins can have unusually large A_2 values.[14] For instance, A_2 for polyethylene in TCB is 3−4 times larger than that for polystyrene with the same molecular weight.[18] The effect of neglecting A_2 in determining M_w may be 5−7% at the elution peak for polyethylene with $M_w \sim 10^5$ and $M_w/M_n \sim 2.0$. Although still second order in importance, it nevertheless seemed desirable to account for its contribution in the data analysis.

Some information about the A_2 contributions can be obtained by running a range of polymer concentrations in the SEC−MALLS system and analyzing the resultant light-scattering intensities. Values of A_2 can be determined in this way although not as reliably as by measurements in a traditional static system because the concentration range is limited (concentrations giving $2A_2Mc \approx 1$ near the SEC peak would overload the columns). However, such data can still be usefully analyzed with the help of dilute solution theory. The product A_2M^2 is a thermodynamic size,[19] describing a volume excluded by a polymer molecule to the other polymer molecules. In good solvents, this size can be correlated with R_g, a quantity that the SEC−MALLS measures well. We used the approximate A_2 values to develop a correlation between $A_2M_w^2$ and the pervaded volume $4\pi N_A R_g^3/3$, where N_A is Avogadro's number, M_w is the weight-average molecular weight of the polymer, and R_g is the value measured by SEC−MALLS at $M = M_w$. Data were obtained for several polymers with three injection concentrations for each. An A_2 value was chosen for each polymer to minimize the apparent concentration dependence of M_w.

A plot of $A_2M_w^2$ vs $4\pi N_A R_g^3/3$ is shown in Figure 2. The following expression is obtained when the fitting line is forced through the origin:

$$A_2 = 1.07\frac{4\pi {R_g}^3 N_A}{3{M_w}^2} \tag{8}$$

Hayward and Graessley[19] examined A_2 and R_g for a series of narrow distribution polymers of several species in various good solvents, all measured at room temperature in a standard goniometer setup. With thermodynamic radius defined by

$$R_T = \left(\frac{3A_2M^2}{16\pi {R_T}^3 N_A}\right)^{1/3} \tag{9}$$

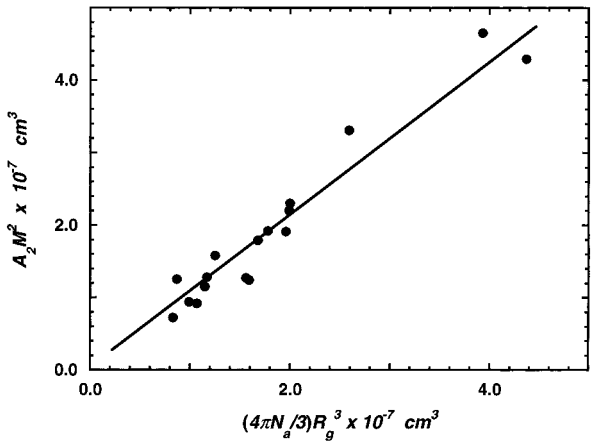

Figure 2. Plot of thermodynamic size vs pervaded volume for various polyolefins in TCB at 135 °C.

they report $R_T = 0.668R_g$; we obtain $R_T = 0.64R_g$ from the results in Figure 2, reassuringly close to their result. We then used that correlation to assign an A_2 value to each polymer based on its R_g and M_w as measured by SEC−MALLS. The second virial coefficient has such a weak molecular weight dependence, $A_2 \propto M^{-0.2}$, that we treated it as a constant throughout the chromatogram.

Huggins Coefficient. From eq 5, k_H is the second-order term in dilute solution viscometry,[13] and its relative importance in interpreting viscometry data is expressed by the product $k_H[\eta]c$. Unfortunately, we were unable to find any values of the Huggins coefficient for polyolefins in TCB, so we merely assigned a good solvent value, $k_H = 0.3$, to all samples. We regard this to be acceptable for two reasons. It is well-known that k_H for linear chains in good solvents is insensitive to M, R_g, and polymer species. Also, even at the height of the elution peak the second-order term $k_H[\eta]c$ is only 0.01−0.02. Thus, the uncertainties in k_H relative to the chosen value are of negligible consequence.

Results

We assume that the molecules in all samples are statistically uniform in structure and long enough for the intermolecular composition fluctuations to have negligible effect. Accordingly, all samples in this study are assumed to behave as linear *polydisperse homopolymers*, such that the SEC fractions derived from each obey the well-established rules for dilute solution behavior of homopolymer fractions. The results for each polymer consists of two sets of data, R_g vs M and $[\eta]$ vs M, obtained from the outputs of the two system configurations. An example of the SEC−MALLS output, R_g and M as functions of retention volume, RV, is shown in Figure 3. The vertical lines indicate the range over which R_g and M are both known. Since determination of M requires knowing the polymer concentration, the DRI signal weakness sets the lower limit in this case; note that the plot of M vs retention volume RV breaks up before the plot of R_g vs RV. The upper limit is determined by the asymmetry in scattering; here R_g vs RV breaks up before M vs RV. Similarly for $[\eta]$ vs M data the DRI signal weakness sets the lower limit; determination of both $[\eta]$ and M depend on concentration, and therefore, $[\eta]$ and M break up simultaneously. The upper limit is determined by the weaker of the LALLS and viscometer signals; typically the LALLS signal is the weaker at the high RV end.

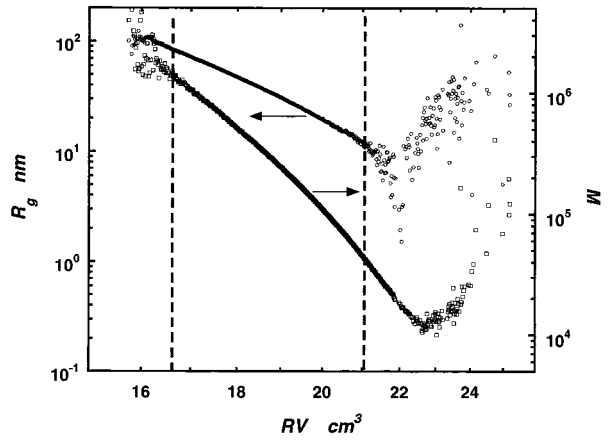

Figure 3. Plots of molecular weight (bottom) and radius of gyration (top) as a function of retention volume for the SEC−MALLS configuration.

For the polymers studied here, both R_g vs M and $[\eta]$ vs M are well described by power laws:

$$R_g = K_s M^{\alpha_s} \tag{10}$$

$$[\eta] = K_v M^{\alpha_v} \tag{11}$$

Results for the $[\eta]-M$ relationship of polyethylene in TCB at 135 °C are compared with the data of three other groups,[20−22] obtained with fractions and employing traditional techniques, in Figure 4a. Here, we converted the quoted bulk M_w values as measured by these groups by light scattering to M_v by assuming a log-normal distribution and using the quoted polydispersities. The exponent obtained with the literature data alone is 0.695, and it changes imperceptibly when our data for HDPE and for NBS1475 are included. The agreement is obviously very good. We were unable to locate corresponding literature results for R_g vs M for polyethylene in TCB, due no doubt to the difficulty of doing light-scattering measurements in traditional goniometer setups at elevated temperatures. In lieu of this, in Figure 4b, we compare results for our linear polyethylene control to those obtained from a subset of the previously mentioned model EB copolymers, all having about 8 wt % butene.[16] To permit direct comparison with the PE control sample, we have adjusted the measured R_g of the EB samples upward by 1.025 to account for the butene content, as described later herein. Again, the agreement is very good.

Results for the ethylene−propylene copolymer series are shown in Figures 5 and 6. Approximately parallel power laws are found, indicating that the power-law exponents are insensitive to the comonomer content. Fitted values for the six samples, averaged over a few runs for each, are 0.579, 0.577, 0.571, 0.590, 0.592, and 0.597 for α_v; 0.701, 0.700, 0.684, 0.688, 0.689, and 0.703 for α_v. The methodology for the power law fits is described in the Appendix, and is based on a weighted least squares procedure designed to account for the errors in R_g, $[\eta]$, and M. Similar plots of data for the five homopolymers in Figures 7 and 8 also show nearly parallel power laws, with exponents similar to those for the copolymers. Fitted values are 0.577, 0.597, 0.610, 0.571 and 0.595 for α_s; 0.700, 0.703, 0.700, 0.690, and 0.703 for α_v.

Average values (typically over 3 or more runs) of α_s and α_v for each of the four copolymer types are listed in

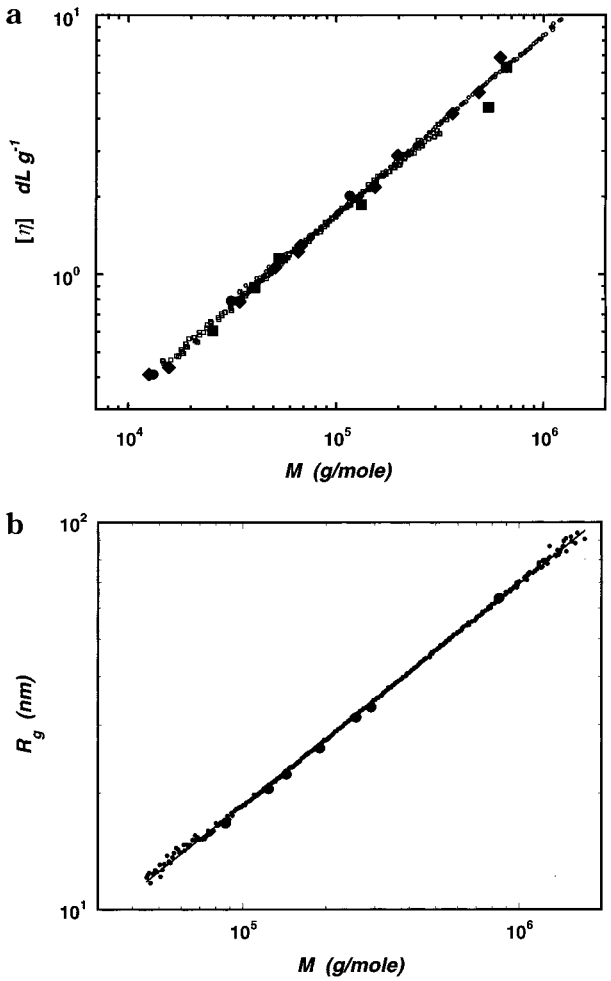

Figure 4. (a) Correlation of intrinsic viscosity with molecular weight for polyethylene in TCB at 135 °C. The symbols indicate data from Wagner and Hoeve[19] (◆), Peyrouset et al.[20] (■), Raju, et al.[21] (●), NBS 1475 (this work, small □) and HDPE (this work, small ○). (b) Correlation of radius of gyration with molecular weight for polyethylene in TCB at 135 °C. The (●) symbols indicate data from a 8 wt % butene subset of the model EB copolymers. The R_g data was adjusted for butene content for better comparison with the polyethylene reference (see text).

Table 3. Size and Viscosity Exponents for the Homopolyethylene and Ethylene Copolymer Species

polymer	α_s	α_v
homopolyethylene	0.579	0.701
EP copolymers	0.585	0.691
EB copolymers	0.572	0.687
EH copolymers	0.576	0.686
EO copolymers	0.587	0.699

Table 3. The sample-to-sample variations are greater for α_s, but we regard both to be similar enough for overall average values to suffice for all polymers. Thus, with negligible effect and considerable simplification in the subsequent analysis, the averaged exponents $\alpha_s = 0.580$ and $\alpha_v = 0.695$ have been imposed on the data for all polymers, making their power-law coefficients, K_s and K_v, directly comparable. The 0.580 exponent for R_g is consistent with measurements made on many other polymers in good solvents[18,23] and close to the theoretical exponent[24] of 0.588. The 0.695 exponent for $[\eta]$ is somewhat smaller than typically found for good solvent systems, but it is within the range of values reported in earlier studies of polyolefins in good sol-

Table 4. Size and Intrinsic Viscosity Power-Law Coefficients and Ratios

polymer	$K_s \times 10^2$ (nm)	$K_v \times 10^4$ (dL/g)	g_{SCB}	g'_{SCB}
HDPE	2.30	5.79	1.000	1.000
EP22	2.18	5.23	0.902	0.905
EP27	2.14	5.07	0.872	0.876
EP52	2.02	4.20	0.774	0.726
EP81	1.83	3.14	0.632	0.542
EP100	1.73	2.62	0.569	0.452
EB8	2.20	5.45	0.922	0.942
EB9	2.19	5.31	0.911	0.918
EB10	2.19	5.30	0.910	0.915
EB11	2.19	5.25	0.906	0.908
EB12	2.18	5.18	0.901	0.895
EB13	2.17	5.14	0.896	0.888
EB18	2.11	4.84	0.846	0.836
EB19	2.17	4.97	0.892	0.859
EB22	2.15	4.82	0.879	0.833
EB25	2.12	4.50	0.852	0.777
EB100	1.52	1.81	0.436	0.313
EH5	2.24	5.56	0.952	0.960
EH6	2.23	5.51	0.946	0.953
EH9	2.20	5.46	0.921	0.944
EH11	2.19	5.24	0.908	0.905
EH12	2.17	5.15	0.894	0.890
EH14	2.16	5.10	0.889	0.882
EH18	2.13	4.91	0.862	0.848
EH70	1.74	2.61	0.577	0.450
EH100	1.44	1.54	0.392	0.266
EO10	2.21	5.48	0.924	0.947
EO13	2.17	5.40	0.897	0.933
EO18	2.18	5.14	0.902	0.888
EO34	2.08	4.22	0.817	0.729
EO42	1.96	3.85	0.728	0.666
EO50	1.85	3.48	0.652	0.602
EO100	1.41	1.31	0.377	0.226

vents.[21,22] The power law coefficients obtained with those exponents are listed in Table 4.

The reproducibility of determining the power law coefficients for a sample depends on its molecular weight and polydispersity. Samples of high molecular weight are advantageous for measuring both R_g and M (as is the case for traditional goniometer and viscometry setups). Large polydispersities are also an advantage since they provide data over an extended molecular weight range. To obtain an estimate of the reproducibility of these techniques we measured the HDPE control numerous times on both the SEC−MALLS and SEC−LALLS−VIS. For this sample, M_w = 182,000 g/mol and $M_w/M_n \sim 4.0$. In 12 runs on the SEC−MALLS, we obtained an average $\alpha_s = 0.58$ with a standard deviation of 0.007. By forcing each of the runs to fit $\alpha_s = 0.58$, we obtain an average $K_s = 2.30 \times 10^{-2}$ with a standard deviation of 2.0×10^{-4}. In 14 runs on the SEC−LALLS−VIS, we obtained an average $\alpha_v = 0.701$ with a standard deviation of 0.008. By forcing each of the runs to $\alpha_v = 0.695$ we obtain an average $K_v = 5.78 \times 10^{-4}$ with a standard deviation of 6.0×10^{-6}.

As a test of internal consistency, and incidentally to validate the effective homopolymer hypothesis, we compare the results in Table 4 with the general R_g−$[\eta]$ relationship for linear homopolymers in good solvents. Thus, a viscometric radius can be calculated from the $[\eta]$−M relationship[18]

$$R_v = \left(\frac{3[\eta]M}{10\pi N_A}\right)^{1/3} \qquad (12)$$

and for a wide range of good solvent systems[18]

$$R_v \approx 0.75R_g \quad 50\,000 < M < 500\,000 \qquad (13)$$

Table 5. Range of the Size Ratio R_v/R_g for the Polymers in This Study

mol weight	av R_v/R_g	range of R_v/R_g
100 000	0.782	0.768−0.800
200 000	0.774	0.763−0.787
300 000	0.769	0.759−0.779

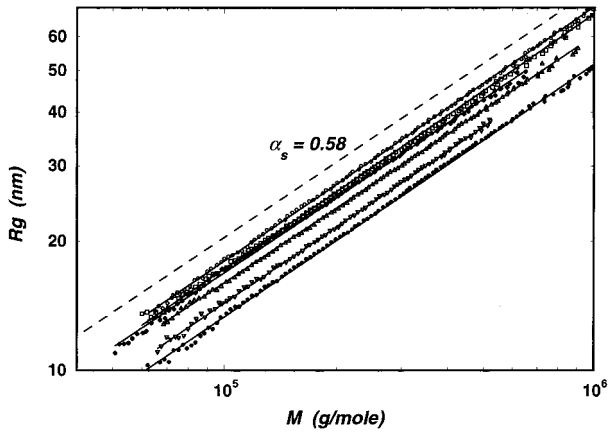

Figure 5. Relationship of radius of gyration and molecular weight for ethylene−propylene copolymers. The symbols in order of upper left line to lower right line indicate the following: HDPE (○), EP22 (□), EP27 (◆), EP52 (△), EP81 (▽), and EP100 (●). The dashed line corresponding to $\alpha_s = 0.58$ serves as a guide to the eye.

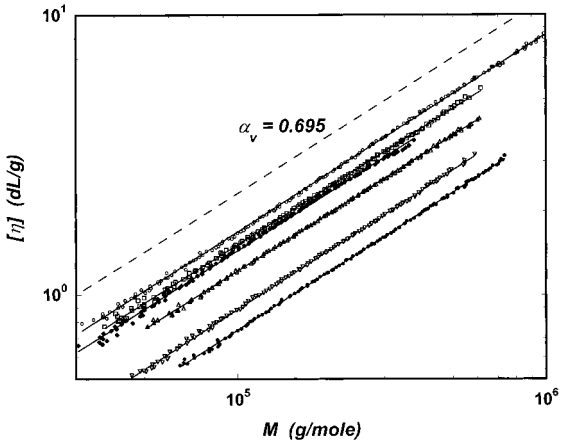

Figure 6. Relationship of intrinsic viscosity and molecular weight for ethylene-propylene copolymers. The symbols in order of upper left line to lower right line indicate the following: HDPE (○), EP22 (□), EP27 (◆), EP52 (△), EP81 (▽), and EP100 (●). The dashed line corresponding to $\alpha_v = 0.695$ serves as a guide to the eye.

The average of R_v/R_g at three molecular weights and the extreme values among the 33 polymers studied are listed in Table 5. Despite the significant range of comonomer types and amounts, essentially the same result is obtained for all. The average ratio, $R_v/R_g = 0.774$ over the ranges covered and even the weak decreasing trend in R_v/R_g with increasing molecular weight are consistent with homopolymer behavior in good solvents.[19]

Discussion of Results

In analyzing the results we define two new parameters, g_{SCB} and g'_{SCB}, to express the effect of short-chain branching, i.e., the comonomer content, on chain dimensions and intrinsic viscosity. Patterned after the pa-

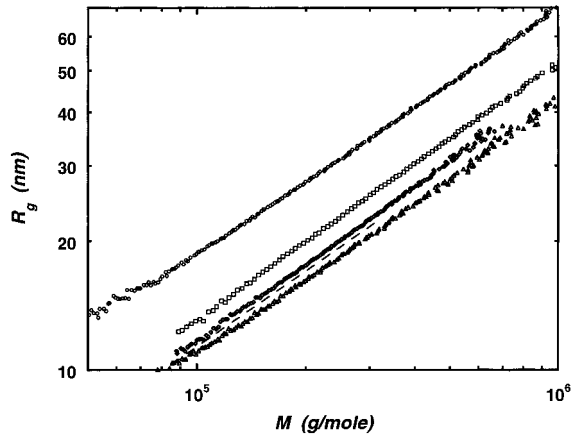

Figure 7. Relationship of radius of gyration and molecular weight for the homopolymers. The symbols in order of upper left line to lower right line indicate the following: HDPE (●), EP100 (□), EB100 (◊), and EO100 (△). For the sake of clarity the EH100 data are represented by the dashed line between EB100 and EO100.

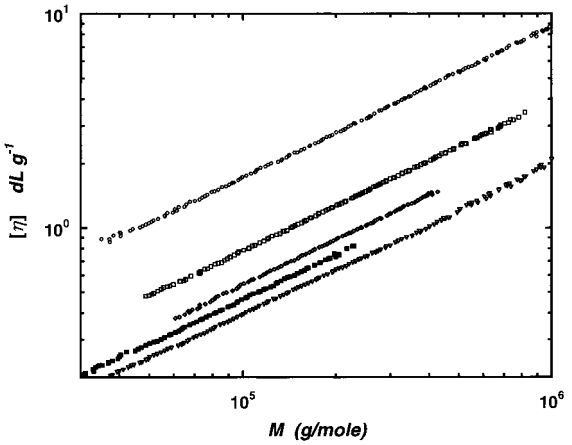

Figure 8. Relationship of intrinsic viscosity and molecular weight for the homopolymers. The symbols in order of upper left line to lower right line indicate the following: HDPE (○), EP100 (□), EB100 (◊), EH100 (■) and EO100 (△).

rameters for long-chain branching, they are

$$g_{\mathrm{SCB}} = \frac{R_g^{\,2}}{(R_g^{\,2})_{\mathrm{L}}} \tag{14}$$

$$g'_{\mathrm{SCB}} = \frac{[\eta]}{([\eta])_{\mathrm{L}}} \tag{15}$$

where the comparisons are made at the same total molecular weight. In this study, the power-law exponents are taken to be the same for all polymers, so the ratios only depend on the coefficients:

$$g_{\mathrm{SCB}} = \frac{K_s^{\,2}}{(K_s^{\,2})_{\mathrm{PE}}} \tag{16}$$

$$g'_{\mathrm{SCB}} = \frac{K_v}{(K_v)_{\mathrm{PE}}} \tag{17}$$

Here, the subscript *PE* refers to the homopolyethylene values. Values of g_{SCB} and g'_{SCB} are listed in Table 4. From the effective linear homopolymer hypothesis and eq 13, the ratios should be related. Thus, we expect the approximate equality

$$(K_s M^{\alpha_s})^3 = \gamma M K_v M^{\alpha_v} \tag{18}$$

where γ is the same for all species over the range of interest. Accordingly, assuming strict adherence to the linear homopolymer hypothesis, we anticipate

$$g'_{\mathrm{SCB}} = g_{\mathrm{SCB}}^{\,3/2} \tag{19}$$

This expected equality is in fact obeyed, within the uncertainties by the independently determined values of g_{SCB} and g'_{SCB} in Table 4: $\langle g'_{\mathrm{SCB}}/g_{\mathrm{SCB}}^{3/2}\rangle = 1.05 \pm 0.05$. Since γ, K_s and K_v in eq 18 are all independent of M, we also expect $\alpha_s = (1 + \alpha_v)/3$. The results in Table 3 agree with this relationship within a few percent.

The values of g_{SCB} and g'_{SCB} for the four series of copolymers are plotted as functions of comonomer weight fraction w in Figures 9−12. The model EB copolymers are included, and although made in an entirely different manner they agree well with the other EB materials. Within the uncertainties of the data, g_{SCB} and g'_{SCB} for all four copolymer series vary linearly with w over the entire range of composition, although the EB data for both g_{SCB} and g'_{SCB} display some curvature in the data. Of course, both g_{SCB} and g'_{SCB} cannot be

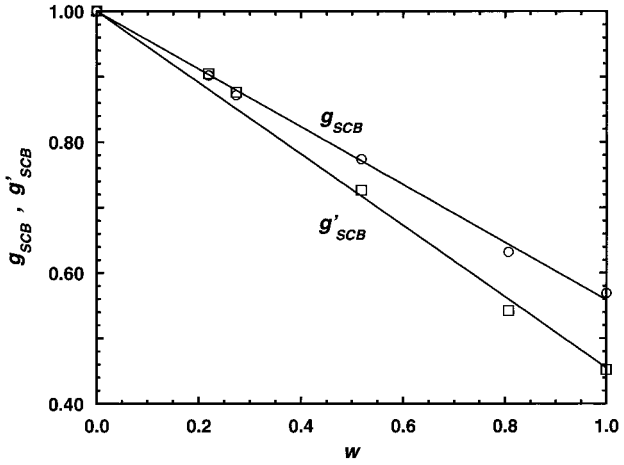

Figure 9. Dependence of radius of gyration ratio and intrinsic viscosity ratio on composition for ethylene−propylene copolymers. The symbols indicate values of g_{SCB} (○) and g'_{SCB} (□).

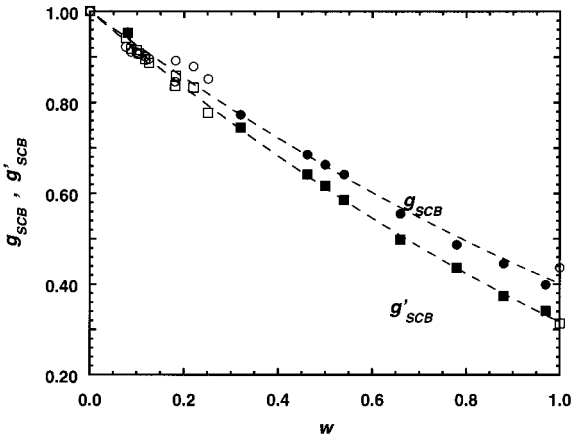

Figure 10. Dependence of radius of gyration ratio and intrinsic viscosity ratio on composition for ethylene−butene copolymers. The symbols indicate values of g_{SCB} (○) and g'_{SCB} (□) for the copolymers and g_{SCB} (●) and g'_{SCB} (■) for the model materials. The dashed lines serve as guides to the eye.

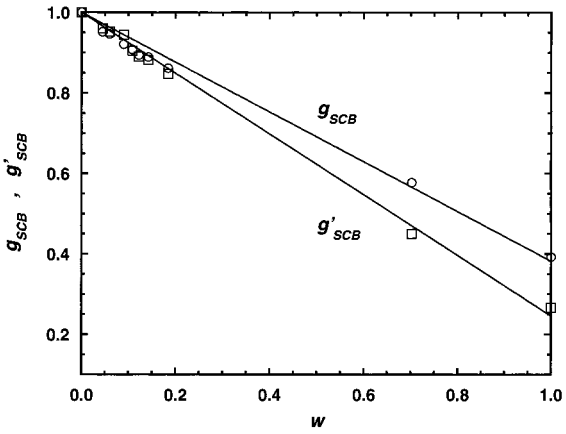

Figure 11. Dependence of radius of gyration ratio and intrinsic viscosity ratio on composition for ethylene−hexene copolymers. The symbols indicate values of g_{SCB} (○) and g'_{SCB} (□).

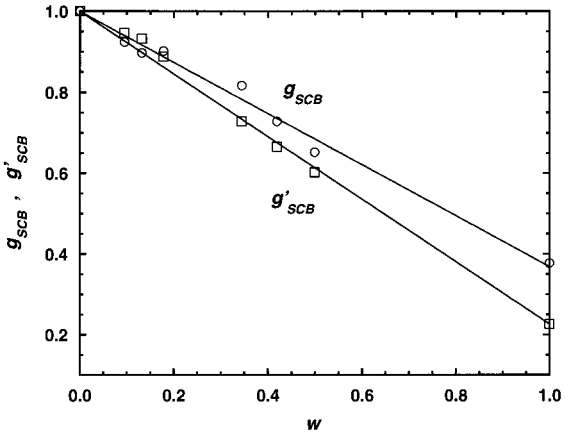

Figure 12. Dependence of radius of gyration ratio and intrinsic viscosity ratio on composition for ethylene−octene copolymers. The symbols indicate values of g_{SCB} (○) and g'_{SCB} (□).

precisely linear in w if eq 19 is literally true. There is also no reason to expect a linear dependence of either g_{SCB} or g'_{SCB} on w, and such simple behavior, even if only approximate, is surprising. Nonetheless, the results, forced through $g_{SCB}(0) = 1$ and $g'_{SCB}(0) = 1$, are reasonably well described by

$$g_{SCB} = 1 - C_s w$$
$$g'_{SCB} = 1 - C_v w \qquad (20)$$

where $C_s = 0.44$, 0.63, 0.62, and 0.63 and $C_v = 0.54$, 0.72, 0.75, and 0.77 for the EP, EB, EH and EO series, respectively. In the case of the EB data, we also applied a curved fit to the data

$$g_{SCB} = 1 + C_{s,1} w + C_{s,2} w^2$$
$$g'_{SCB} = 1 + C_{v,1} w + C_{v,2} w^2 \qquad (21)$$

and obtain −0.76, 0.16, −0.87, and 0.18 for $C_{s,1}$, $C_{s,2}$, $C_{v,1}$, and $C_{v,2}$ respectively.

It has occasionally been proposed[25] that the effect of comonomer composition and type on R_g and $[\eta]$ in the copolymers of ethylene with α-olefins can be explained simply by considerations based on backbone length alone.[25] Thus, the incorporation of comonomer brings in the extra mass of the side group and would thereby alter the relationships of R_g and $[\eta]$ to M. The following formula describes the effect of copolymerization on size according to the backbone model

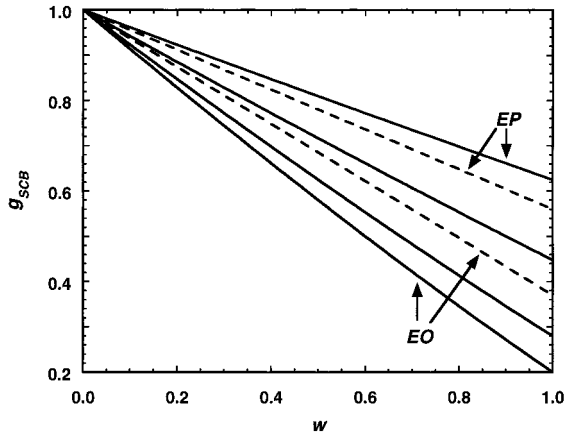

Figure 13. Comparison of observed radius of gyration ratios (- - -) with predictions of the backbone model (—).

$$g_{SCB} = \left[1 - \frac{X-1}{X} w\right]^{1.16} \qquad (22)$$

in which $X = m_{CO}/m_E$, the ratio of comonomer to ethylene molecular weight, is 1.5, 2.0, 3.0, and 4.0 for EP, EB, EH, and EO, respectively. The exponent of 1.16 is $2\alpha_s$ with $\alpha_s = 0.58$.

The backbone model predictions are shown in Figure 13 along with lines representing g_{SCB} data for the EP, EH and EO series. The decrease in g_{SCB} is larger than predicted for the EP series, a discrepancy that is qualitatively consistent with the known reduction in persistence length from polyethylene to polypropylene.[26] The trend reverses for larger side groups, the reduction predicted by the backbone model being larger than observed for the EH and EO series. The observed behavior is consistent with suggestions that persistence length begins to increase again owing to increased side group crowding.[27,28] Thus, factors of a more detailed structural nature than envisioned by the backbone model are also important. Although the model has some qualitative value, it is inappropriate for use when quantitative estimations are required.

Acknowledgment. We gratefully acknowledge A. Faldi, B. Chapman, D. Higgins, V. Johnson, C. Pavlick, J. Poffenbarger, and L. Soni for their assistance in this work. We also acknowledge D. Lohse, S. Datta, B. Harrington, and N. Merrill for providing relevant samples and B. Harrington for the FTIR analysis of the EP copolymers.

Appendix: Error Analysis for R_g, $[\eta]$, M, and Power Law Fits

We start by assigning an error to each of the chromatogram signals (all MALLS, LALLS, viscometry, and DRI signals). This error is determined by fitting a line through the first 100 (near baseline) points in each chromatogram. The assigned error is the standard deviation about this line. For analysis of SEC−MALLS data we start with the assigned chromatogram errors and use standard error analysis to determine the error in the term $(K_o c/\Delta R(\theta) - 2A_2 C)$. We then use a Levenberg−Marquardt least-squares fit to determine both M and R_g, and their fit errors.[29] For analysis of SEC−

LALLS−VIS data, which does not require a least-squares fit, we use standard error propagation analysis to determine the error in M and $[\eta]$. Having determined the errors in M, R_g, and $[\eta]$, we then iteratively fit for the scaling laws weighing each point inversely according to its fit error. In the first iteration we use only the error in the coil dimension term (R_g *or* $[\eta]$); upon subsequent iterations, we use an "effective" error, σ, based on the error in coil dimension combined with the error in M:

$$\sigma^2 = \Delta R_{g,fit}{}^2 + \Delta R_{g,M}{}^2$$

Here, $\Delta R_{g,fit}{}^2$ is the above-described fit error in $R_g{}^2$, and $\Delta R_{g,M}$ is given by $K_s\alpha_s M^{\alpha-1} \times \Delta M$ where K_s and α_s are the power law parameters determined in the previous iteration and ΔM is the error in M. A similar routine is used for fitting the $[\eta]$ vs. M data.

References and Notes

(1) Mandelkern, L. Chapter 4 In *Physical Properties of Polymers*, 2nd ed.; Mark, J. E., et al., Eds.; American Chemical Society: Washington, DC, 1993.
(2) Ward, I. M. *Mechanical Properties of Solid Polymers*, 2nd ed.; J. Wiley & Sons: New York, 1983.
(3) Randall, J. *Polymer Sequence Determination: Carbon-13 NMR Method*; Academic Press: New York, 1977.
(4) Koenig, J. L. *Spectroscopy of Polymers*; American Chemical Society: Washington, DC, 1992.
(5) Wild, L. *Adv. Polym. Sci.* **1990**, *98*, 1.
(6) Barth, H. G., Mays, J. Eds. *Modern Methods of Polymer Characterization*; J. Wiley & Sons: New York, 1991.
(7) Wu, C.-S., Ed. *Handbook of Size Exclusion Chromatography*; Dekker: New York, 1995.
(8) Cotts, P. M.; Guan, Z.; McCord, E.; McLain, S. *Macromolecules* **2000**, *33*, 6945.
(9) Kaminski, W.; Arndt, M. *Adv. Polym. Sci.* **1997**, *127*, 143.
(10) Wagner, H. L.; Verdier, P. H. *NBS J. Res.* **1972**, *76A*, 137.
(11) NIST Certification Sheets for NBS1482, NBS1483, and NBS1484.
(12) Huglin, M. B. *Light Scattering from Polymer Solutions*; Academic Press: New York, 1972.
(13) Yamakawa, H. *Modern Theory of Polymer Solutions*, Harper & Row: New York, 1971.
(14) Pope, J. W.; Chu, B. *Macromolecules* **1984**, *17*, 2633.
(15) Graessley, W. W.; Krishnamoorti, R.; Balsara, N. P.; Butera, R. J.; Fetters, L. J.; Lohse, D. J.; Schulz, D. N.; Sissano, J. A *Macromolecules* **1994**, *27*, 3896.
(16) Manuscript in preparation.
(17) Han, S. J.; Lohse, D. J.; Condo, P. D.; Sperling, L. H. *J. Polym. Sci., Polym. Phys. Ed.* **1999**, *37*, 2835.
(18) Davidson, N. S.; Fetters, L. J.; Funk, W. G.; Hadjichristidis, N.; Graessley, W. W. *Macromolecules* **1987**, *20*, 2614.
(19) Hayward, R. C.; Graessley, W. W. *Macromolecules* **1999**, *32*, 3502.
(20) Wagner, H. L.; Hoeve, C. A. J. *J. Polym. Sci.* **1973**, *11*, 1189.
(21) Peyrouset, A.; Prechner, R.; Panaris, R.; Benoit, H. *J. Appl. Polym. Sci.* **1975**, *19*, 1363−1371.
(22) Raju, V. R.; Smith, G. G.; Marin, G.; Knox, J. R.; Graessley, W. W. *J. Polym. Sci.: Polym. Phys. Ed.* **1979**, *17*, 1183.
(23) Fetters, L. J.; Hadjichristidis, N.; Lindner, J. S.; Mays, J. W. *J. Phys. Chem. Ref. Data* **1994**, *23*, 619.
(24) Le Guillou, J. C.; Zinn-Justin, J. *Phys. Rev. Lett.* **1977**, *39*, 95.
(25) Scholte, Th. G.; Meijerink, N. L. J.; Schoffeleers, H. M.; Brands, A. M. G. *J. Appl. Polym. Sci.* **1984**, *29*, 3763.
(26) Fetters, L. J.; Graessley, W. W.; Krishnamoorti, R.; Lohse, D. J. *Macromolecules* **1997**, *30*, 4973.
(27) Wang, J.-S.; Porter, R. S.; Knox, J. R. *Polym. J.* **1978**, *10*, 619.
(28) Sundararajan, P. R. Chapter 15 In *Physical Properties of Polymers Handbook*; Mark, J. E., Ed.; American Institute of Physics, Woodbury, NY, **1996**.
(29) Press, W. H.; Flannery B. P.; Teukolsky, S. A.; Vettering, W. T., *Numerical Recipes*; Cambridge University Press: Cambridge, England, 1986.

MA010718E